

Cyclic Fatigue Due to Electric Loading in Ferroelectric Ceramics

H. Weitzing,^{a*} G. A. Schneider,^a J. Steffens,^a M. Hammer^b and M. J. Hoffmann^b

^aAdvanced Ceramics Group, Technical University Hamburg-Harburg, Germany

^bInstitute for Ceramics in Mechanical Engineering, University of Karlsruhe, Germany

Abstract

Mechanical fatigue of ferroelectric ceramics due to bipolar cyclic electric loading is examined. Beam specimens out of three different PZT materials were cut and precracks were initiated by Vickers indentation. The specimens were loaded by alternating electric fields varied from 0.9 to 1.0 and 1.5 times the coercive field E_c . In short intervals the crack propagation was measured. Before and after fatigue experiments electric polarisation and strain were measured as a function of the electric field. The crack growth rate decreases with increasing cycle number, and a saturation point is reached after approximately 10^5 cycles. A correlation between growth rates and ferroelectric strain was detected. Measured strain loops suggest that switching of ferroelectric domains undergoes a strong fatigue effect. Therefore after 10^6 cycles the elastic strain is not as strong a driving force for further crack extension. In addition fatigue-crack growth is strongly dependent on the material and the electric field strength. © 1999 Elsevier Science Limited. All rights reserved

Keywords: fatigue, ferroelectric properties, PZT.

1 Introduction

Ferroelectric materials are used for a broad range of applications such as voltage generators, transducers, sensors and filters.^{1–3} Owing to their quick response times, high force generation, and precise displacement control they are especially suitable for use as micropositioners in fuel injection systems.⁴ However, high alternating electric fields cause mechanical and electrical degradation of

ferroelectrics.^{5–8} Electrical-induced mechanical fatigue-cracking is a serious degradation phenomenon which is not yet understood. In this study fatigue due to cyclic electric loading by an alternating field was examined. Fatigue-crack propagation for rhombohedral and morphotropic PZT materials was measured and related to the degradation of the ferroelectric properties in order to improve understanding of fatigue processes.

2 Experimental

2.1 Cyclic electric fatigue

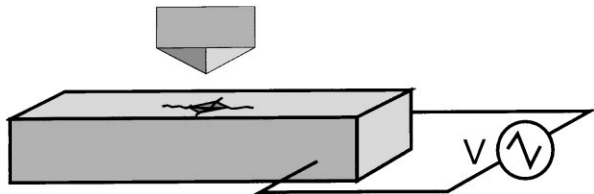
Three different PZT materials⁹ were used for cyclic fatigue experiments. One rhombohedral composition and two morphotropic compositions where the grain size was varied (Table 1). Beam specimens with the dimension $17 \times 2.6 \times 2.3 \text{ mm}^3$ were cut, polished on one face, and silver electrodes were applied onto the faces perpendicular to the polished side. Precracks perpendicular to the electric field were initiated by Vickers indentation with a load of 19.6 N for 20 s (Fig. 1). The cracks emanating from the indentation were measured using an optical microscope. After that the specimens were loaded cyclically using a bipolar electric signal of triangular waveform at frequencies of 50, 100, 200, and 500 Hz. The specimens were cycled in silicon oil in order to prevent electrical discharge and subcritical crack growth. Since domain switching is expected to cause fatigue-cracking, the amplitude of the cycling field E_{cycle} was adjusted to three values relative to the coercive field E_c . Values used were $E_{\text{cycle}} = 0.9, 1.0, \text{ and } 1.5 \text{ times } E_c$.

Fatigue-crack propagation was measured in short intervals using an optical microscope. After 10^6 cycles at high electric fields ($1.5 \times E_c$) or 10^7 at low fields ($0.9 \times E_c$) experiments were stopped and the specimens' ferroelectric properties were measured.

*To whom correspondence should be addressed. Fax: +49-040-7718-2647; e-mail: weitzing@tu-harburg.de

Table 1. PZT compositions used for fatigue experiments

| Material system | Zr/Ti ratio | Dopants | Phase composition | Average grain size (μm) | Name |
|-----------------|-------------|-----------|-----------------------------|--------------------------------------|------------|
| PZT | 54/46 | 2% mol La | Morphotropic phase boundary | 1.87 | MPB fine |
| PZT | 54/46 | 2% mol La | Morphotropic phase boundary | 3.29 | MPB coarse |
| PZT | 60/40 | 2% mol La | Rhombohedral | 1.82 | Rhom fine |

**Fig. 1.** Experimental set-up for the determination of fatigue-crack propagation.

2.2 Ferroelectric properties

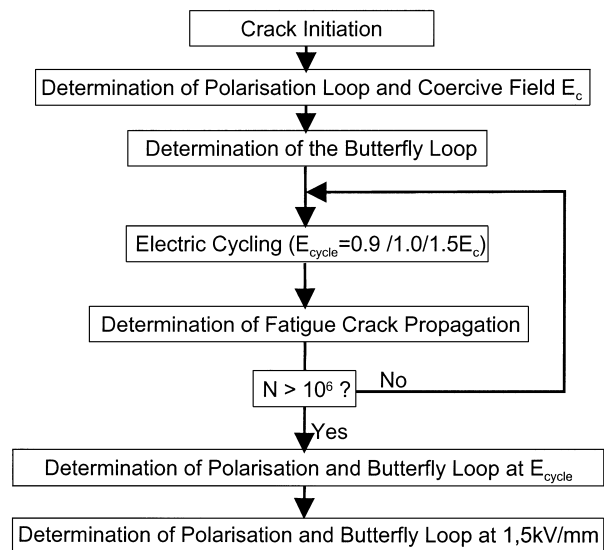
Before cycling the ferroelectric properties of each specimen were determined. A Sawyer-Tower-Circuit was used to measure the electrical polarization as a function of the electric field. Thus the coercive field, E_c , was determined. The strain hysteresis ('butterfly') loop was measured as well, and the maximum strain for bipolar loading at 1.5 kV mm^{-1} was quantified.

In order to characterise the fatigue effect butterfly loops were measured before and after cycling with maximum electric fields corresponding to E_{cycle} , respectively. By this means the fatigue behaviour was determined. Finally, the butterfly loops of the cycled specimens were measured with a maximum electric field of $E = 1.5 \text{ kVmm}^{-1}$. The experimental procedure is shown in Fig. 2.

3 Results

3.1 Fatigue-crack propagation

All three PZT compositions show fatigue-crack propagation due to cyclic electric loading. The crack extension as a function of the cycling field $E_{\text{cycle}} = 0.9E_c$ and $1.5E_c$ is shown in Fig. 3. Experiments at $E_{\text{cycle}} = 0.9$ and $1.0E_c$ show qualitatively the same results except that crack extensions at $1.0E_c$ are higher by a factor of two. For better clearness the results for $E_{\text{cycle}} = E_c$ are not included in Fig. 3. Bipolar electric loading at $E_{\text{cycle}} = 1.5E_c$ causes high fatigue-crack growth with maximum crack extension rates of 10^{-7} – 10^{-8} m/cycle. The material with the highest maximum strain shows the highest crack extension rate. The extension rate decreases with the number of cycles and crack

**Fig. 2.** Experimental procedure for fatigue experiments.

growth stops after 10^5 – 10^6 cycles. At $E_{\text{cycle}} = 0.9E_c$ fatigue-crack propagation is less than $100 \mu\text{m}$ after 10^7 cycles. Extension rates are smaller than 10^{-11} m/cycle. Increasing the frequency of electric loading sometimes causes abrupt crack growth. Changes of frequency are marked by dotted vertical lines.

3.2 Degradation of ferroelectric properties due to fatigue

The peak to peak strain at different values of the electric fields for uncycled and cycled specimens is shown in Table 2. Bipolar cyclic electric loading leads to a strong decrease of strain both at fields above and below coercive field strength. All three examined materials show qualitatively the same behaviour. In Fig. 4 the butterfly loops of the coarse grained morphotropic PZT-composition are shown. Figure 4(a) and (b) show butterfly loops of uncycled specimens whereas Fig. 4(c) and (d) show the results after cycling at a field $E_{\text{cycle}} = 1.5E_c$. The applied field of $E = 1.5 \text{ kV/mm}$ [Fig. 4(d)] is about 18% higher than E_{cycle} .

Before cycling the butterfly loop clearly shows the switching of the electric polarization and a maximum strain of 2.5 and 2.2‰ at $E = 1.5 \text{ kVmm}^{-1}$ and E_{cycle} , respectively. Cyclic electric loading causes the right wing of the

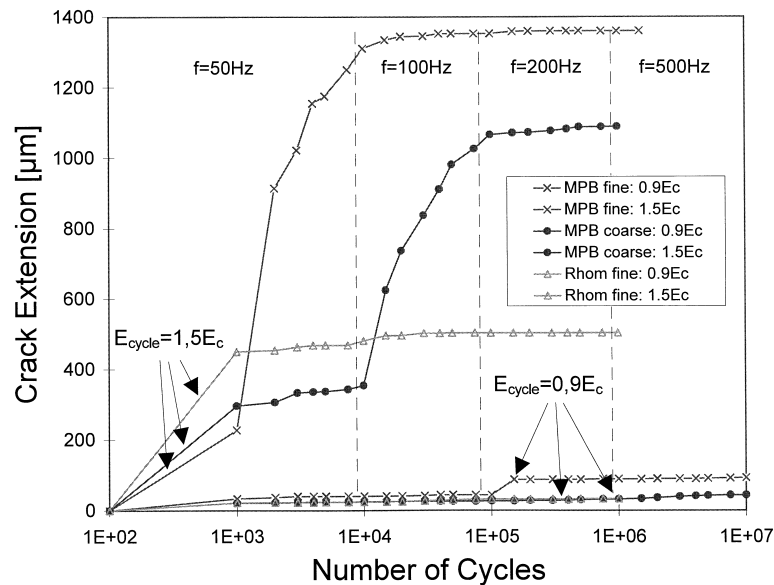


Fig. 3. Crack extension as a function of the number of cycles.

Table 2. Ferroelectric properties of PZT specimens before and after cyclic fatigue

| | E_c ($kV\ mm^{-1}$) | $Strain_{p-p}$ (%) | $Strain_{p-p}$ (%) | $Strain_{p-p}$ (%) | $Strain_{p-p}$ (%) | $Strain_{p-p}$ (%) | $Strain_{p-p}$ (%) |
|-----------------------------|----------------------------|--------------------------|---------------------------------------|--------------------------|---------------------------------------|--------------------------------|---|
| Electric field Condition | | $E = 1.5E_c$ Uncycled | $E = 1.5E_c$ Cycled at $1.5E_c$ | $E = 0.9E_c$ Uncycled | $E = 0.9E_c$ Cycled at $0.9E_c$ | $1.5\ kV\ mm^{-1}$ Uncycled | $1.5\ kV\ mm^{-1}$ Cycled at $1.5E_c$ |
| MPB fine | 0.96 | 2.3 | Defect | 1.3 | 0.7 | 2.8 | Defect |
| MPB coarse | 0.85 | 2.2 | 1.4 | 1.4 | 0.3 | 2.5 | 2.4 |
| Rhom fine | 0.92 | 1.6 | 0.9 | 0.9 | 0.6 | 1.8 | 1 |

butterfly loop to collapse and results in a decrease of strain down to 1.4%. Changing the poling direction of the electric field from negative to positive leads to depoling of the material. However, polarization switching into the positive field direction does not occur. If a negative field is applied again the material is poled anew in that direction. Attached to an alternating electric field of higher strength than E_{cycle} the specimens again show a full butterfly loop and polarization switching.

In addition to the mechanical degradation a shift of the butterfly loop of approx. $0.1\ kV\ mm^{-1}$ into electric positive direction is detected indicated by the dotted lines in Fig. 4(b) and (d). This shift occurs before cycling and remains stable during the whole fatigue test.

4 Discussions and Conclusions

Bipolar cyclic electric loading of PZT-ceramics causes fatigue-crack growth. The crack extension rate correlates with the applied electric field strength and the maximum strain of the material. High electric loads and high strains cause high crack extension rates. Therefore we assume that the

mechanical strain due to electromechanical coupling is the main crack driving force. Since the strain of the specimens decreases because of cyclic electric loading crack propagation decreases, as well. It is important to note that in all cases the crack propagation comes to a standstill which is a requirement for long term reliability.

Since the mechanical strain is assumed to be the main crack driving force it is important to examine the evolution of the butterfly loop due to cyclic fatigue. The most obvious result of cyclic fatigue is the asymmetry of the butterfly loop including the collapse of its right wing. This phenomenon is caused by two different processes. First, the whole loop is shifted to the right into the electric positive direction. We assume that one of the reasons for this shift is the existence of an internal bias field of approx. $0.1\ kV\ mm^{-1}$ inside the ceramic. Therefore the effective electric field inside the specimen as a superposition of external applied field and internal bias field is asymmetric. The electro-mechanical coupling consequently leads to an asymmetry of the butterfly loop. An internal bias field of $0.1\ kV\ mm^{-1}$, however, does not shift the positive coercive field far enough as to prevent domains from switching and therefore cause the

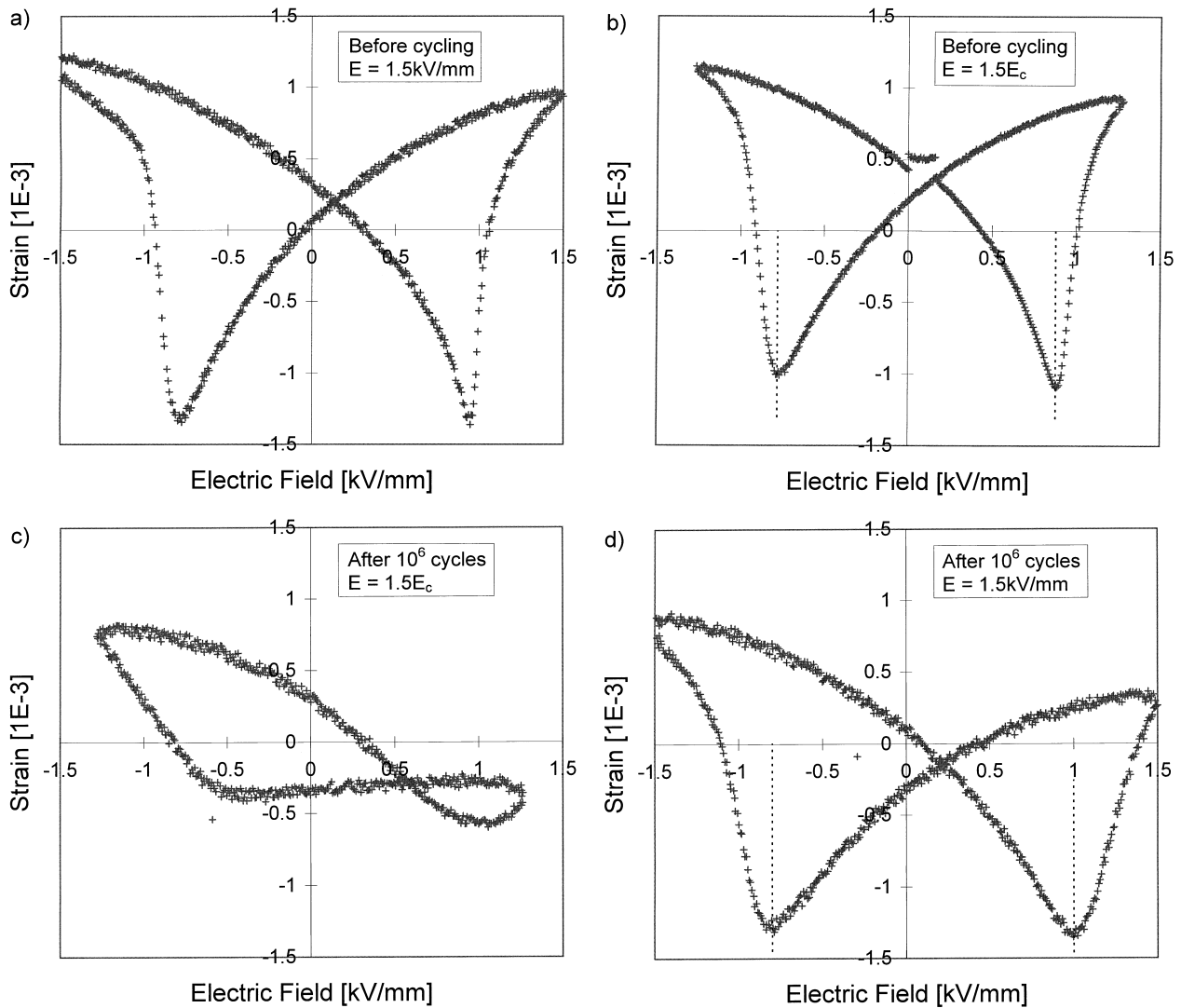


Fig. 4. Ferroelectric properties of the MPB coarse grained material: (a) and (b) before cycling measured at $E = 1.5 \text{ kVmm}^{-1}$ and $E = 1.5E_c$ respectively; (c) and (d) after 10^6 cycles measured at $E = 1.5E_c$ and $E = 1.5 \text{ kVmm}^{-1}$, respectively.

right wing of the butterfly loop to collapse. That leads to the conclusion that, secondly, cyclic fatigue strongly impedes switching of domains. Domain walls are pinned so that the domains remain in a preferred poling direction which leads to degradation of the materials ferroelectric properties. With little ferroelectric switching the linear inverse piezoelectric effect causes most of the mechanical strain of cycled specimens [see Fig. 4(c)] which leads to the collapse of the right wing of the butterfly loop. In addition the peak to peak strain of cycled specimens is much smaller compared to uncycled specimens.

In Fig. 4(d) the butterfly loop of a specimen after 10^6 cycles is shown. An electric field of 1.5 kV mm^{-1} which is 18% higher than E_{cycle} was attached. The degradation of ferroelectric properties is reversed by the reactivation of the switching processes. This can be clearly seen as the right wing of the loop develops again. That leads to the conclusion that cyclic fatigue at a given electric load causes no

irreversible material damage if a boundary value for the mechanical strain is not exceeded.

Future experiments are planned in order to investigate on the development of the internal bias field and the degradation of ferroelectric properties.

Acknowledgements

The authors gratefully acknowledge support by the German Science Foundation (DFG).

References

1. Swartz, S. L., Topics in electronic ceramics. *IEEE Trans. on Electrical Insulation*, 1990, **25**, 935–987.
2. Newnham, R. E. and Ruschau, G. R., Smart electroceramics. *J. Am. Ceram. Soc.*, 1991, **74**(3), 463.
3. Moulson, H., *Electroceramics*, Chapman and Hall, London, 1990.
4. Dürnholtz, M. et al., Piezoelektrisch gesteuertes Einspritz

- system zur Verbesserung des Emissionsverhaltens von direkteinspritzenden Dieselmotoren, 14. Int. Wiener Motorensymposium. VDI Verlag, 1993.
5. Furata, A. and Uchino, K., Dynamic observation of crack propagation in piezoelectric multilayer actuators. *J. Am. Ceram. Soc.*, 1993, **76**(6), 1615–1617.
 6. Suo, Z., Mechanics concepts for failure in ferroelectric ceramics, *Smart Struct. and Mat.*, ASME, 1991.
 7. Schneider, G. A. *et al.*, Crack growth in ferroelectric ceramics under mechanical and electrical loading, In *Proceedings of Electroceramics IV*, ed. R. Waser *et al.* Augustinus Buchhandlung, Aachen, 1994, p. 1211–1216.
 8. Cao, H. and Evans, A. G., Electric-field-induced fatigue crack growth in piezoelectrics. *J. Am. Ceram. Soc.*, 1994, **77**(7), 1783–1786.
 9. Hammer, *et al.* Correlation of surface texture and chemical composition in undoped, hard and soft PZT ceramics; *J. Am. Ceram. Soc.*, **81**(3), 1998, 721–724.